

Quasi-phase-matching of high-order-harmonic generation using multimode polarization beating

Lewis Z. Liu,* Kevin O’Keeffe, and Simon M. Hooker
*Clarendon Laboratory, University of Oxford Physics Department,
 Parks Road, Oxford OX1 3PU, United Kingdom*
 (Dated: February 22, 2013)

The generalization of polarization beating quasi-phase matching (PBQPM) and of multi-mode quasi-phase matching (MMQPM) for the generation of high-order harmonics is explored, and a novel method for achieving polarization beating is proposed. If two (and in principle more) modes of a waveguide are excited, modulation of the intensity, phase, and/or polarization of the guided radiation will be achieved; by appropriately matching the period of this modulation to the coherence length, quasi-phase-matching of high harmonic radiation generated by the guided wave can occur. We show that it is possible to achieve efficiencies with multi-mode quasi-phase matching greater than the ideal square wave modulation. We present a Fourier treatment of QPM and use this to show that phase modulation, rather than amplitude modulation, plays the dominant role in the case of MMQPM. The experimental parameters and optimal conditions for this scheme are explored.

Please note that this is an arXiv version of the original APS paper. Please cite original paper L. Z. Liu, K O’Keeffe, and S. M. Hooker, Phys. Rev. A 87, 023810 (2013). APS link here: <http://pra.aps.org/abstract/PRA/v87/i2/e023810>

PACS numbers: 42.55.Vc 42.81.Gs 42.65.Ky

I. INTRODUCTION

High harmonic generation (HHG) is a nonlinear process that enables the production of tunable, coherent soft x-rays with applications in time-resolved science [1–3], ultrafast holography [4], or diffractive imaging [5]. An important feature of HHG is that it is simple to achieve: focusing driving laser radiation to an intensity of order 10^{14} W/cm² in a gaseous target yields coherent radiation with frequencies corresponding to the odd harmonics of the driving radiation ω . A semi-classical theory of this phenomena has been developed by Corkum [6] and a quantum treatment has been given by Lewenstein et al. [7].

However, without additional techniques, HHG is highly inefficient – with a typical conversion ratio of 10^{-6} for generating photons of energy in the 100 eV range, and 10^{-15} for generating 1 keV photons. This low efficiency is partially due to fact that the driving field and the harmonic field have different phase velocities. As a consequence a phase difference develops between the driving field and harmonics generated at each point in the generating medium; this in turn causes the intensity of the generated harmonics to oscillate with distance between zero and some maximum value along the direction of propagation, z . The phase velocity difference is characterized by the wave vector mismatch, Δk , which arises from neutral gas, plasma, and waveguide dispersion; it is given by $\Delta k = k(q\omega) - qk(\omega)$ where q is the harmonic and $k(\omega)$ is the propagation constant for radiation of angular frequency ω . The distance it takes for the two fields to slip in phase by π is the coherence length $L_c = \pi/\Delta k$.

One way of avoiding the phase-mismatch problem is to balance the dispersion so that $\Delta k = 0$, a situation we will describe as “true phase-matching” in order to distinguish it from the quasi-phase-matching discussed below. With true phase-matching – assuming absorption can be neglected – the intensity of the harmonics grows quadratically with the propagation distance z [8–10]. With long wavelength drivers for phase matching, conversion efficiency can be achieved up to 10^{-3} for the VUV region and 10^{-6} in the x-ray region [10]. However, without long wavelength drivers, true phase-matching can only be achieved for relatively low-order harmonics – corresponding to low photon energies – since at the higher driving intensities required to generate high-order harmonics the dispersion becomes dominated by the free electrons and cannot be balanced by the other terms [8]. For higher-order harmonics, so-called quasi-phase-matching (QPM) may be employed in which the harmonic generation is suppressed in the out of phase zones, enabling monotonic growth of harmonic intensity as a function of z . Techniques for QPM include counter-propagating pulses [11–15], multi-mode beating [16–19], and modulated waveguides [20].

Multi-mode QPM (MMQPM) relies on coupling in two or more waveguide modes [16–18]. If the two modes travel at different phase velocities, then the intensity will beat along the propagation length, thereby modulating harmonic generation resulting in QPM. In this paper, we investigate the effect on HHG of the modulation in both the intensity *and* phase of the beating driving radiation. We show that under certain conditions, phase modulation due to mode beating enables harmonics to be generated with greater efficiency than ideal square-wave QPM modulation. Moreover we show that MMQPM is dominated by modulation of the phase, rather than the intensity, of the driving radiation – an effect which was

* L.Liu1@physics.ox.ac.uk

not considered in our earlier analysis [16–18].

Recently we have proposed a new class of QPM based on modulation of the polarization state of the driving radiation within a hollow core waveguide [21–24]. Here we discuss one example of polarization-control QPM: polarization beating QPM (PBQPM) [21, 23]. In this approach, a linear birefringent system modulates the polarization of the driving pulse between linear and elliptical. Because harmonic generation is suppressed for elliptically polarized light, QPM can be achieved if the period of the polarization beating is suitably matched to the coherence length. This paper describes a generalization of MMQPM and PBQPM which combines these two schemes: multi-mode polarization beating quasi-phase matching (MMPBQPM), which utilizes beating between two waveguide modes to modulate the intensity, phase, and/or polarization of the guided radiation. These modulations can lead to QPM if the coherence length L_c of the harmonic generation is appropriately matched to the beat length, L_b , which is the distance it takes for the two modes to develop a phase difference of π . In addition to controlling the relative input polarizations of the two modes, the relative polarization angle between the two modes can also be controlled. This increased parameter space affords greater opportunities for QPM.

In addition we further analyze MMPBQPM using a Jacobi-Anger and Fourier decomposition which affords additional insight into the processes leading to QPM. Similar Fourier techniques used to analyze quasi-phase matching for HHG can be found in [25, 26].

The paper is organized as follows: in Sec. II, the equations for MMPBQPM are derived for two modes, Sec III presents the the Jacobi-Anger and Fourier analytical analysis, and Sec. IV discusses numerical simulation results.

II. DERIVATION OF THE ENVELOPE EQUATION

A. Mode Propagation Equations

In this section, we develop the set of general mode propagation equations for two linearly polarized modes with azimuthal symmetry. If we assume that two modes are excited, then within the waveguide the electric field may be written in cylindrical coordinates as,

$$\vec{\mathcal{E}}(r, z) = E_0 \left\{ c_1 \vec{E}_1(r) e^{i[(\beta_1 + i\alpha_1)z - \omega t]} + c_2 \vec{E}_2(r) e^{i[(\beta_2 + i\alpha_2)z - \omega t]} \right\} \quad (1)$$

where r is the radial coordinate from the propagation axes, \vec{E}_1 and \vec{E}_2 are the normalized transverse electric fields of the driving mode $m = 1$ and modifying mode $m = 2$ respectively, E_0 is the electric field amplitude constant, β_m and α_m are the propagation constant and damping rate of mode m , and ω is the angular frequency of the driving radiation.

Here, the polarizations of the modes $m = 1$ and $m = 2$ are respectively taken to be parallel to, and at an angle Ω , to the x-axis:

$$\vec{E}_1(r) = \begin{pmatrix} M_1(r) \\ 0 \end{pmatrix} \quad (2)$$

$$\vec{E}_2(r) = \begin{pmatrix} M_2(r) \cos(\Omega) \\ M_2(r) \sin(\Omega) \end{pmatrix} \quad (3)$$

where $M_m(r)$ is the normalized transverse electric field profile for the m th mode.

At time $t' = t + \Delta t$, where $\Delta t = -\beta_1/\omega z$, the electric field components are given by,

$$\Re \left[\begin{pmatrix} \mathfrak{E}_x \\ \mathfrak{E}_y \end{pmatrix} \right] = E_0 \begin{pmatrix} c_1 M_1(r) \cos(\omega t') \\ 0 \end{pmatrix} + E_0 \begin{pmatrix} c_2 M_2(r) \cos(\Omega) \cos(\omega t' + \Delta\beta z) \\ c_2 M_2(r) \sin(\Omega) \cos(\omega t' + \Delta\beta z) \end{pmatrix}. \quad (4)$$

where $\Delta\beta = \beta_1 - \beta_2$, and the beat length $L_b = \pi/(\Delta\beta)$.

From this, the values of t' corresponding to the maximum and minimum electric field amplitudes can be found, from which the ellipticity is given by,

$$\varepsilon(r, z) = \sqrt{\frac{\Re\{\mathfrak{E}[t'_{max}(r, z); r, z]\}^2}{\Re\{\mathfrak{E}[t'_{min}(r, z); r, z]\}^2}} \quad (5)$$

where $\Re[\mathfrak{E}]^2 = \Re[\mathfrak{E}_x]^2 + \Re[\mathfrak{E}_y]^2$, and the angle of the major axis is given by,

$$\Theta(r, z) = \tan^{-1} \left(\frac{\Re[\mathfrak{E}_y][t'_{max}(r, z); r, z]}{\Re[\mathfrak{E}_x][t'_{max}(r, z); r, z]} \right). \quad (6)$$

It is useful to note that the relative relative intensity of the driving wave at any given point is given as:

$$I(r, z) = \mathfrak{E}_x(r, z) \mathfrak{E}_x^*(r, z) + \mathfrak{E}_y(r, z) \mathfrak{E}_y^*(r, z) \quad (7)$$

$$\approx c_1^2 M_1^2 + c_2^2 M_2^2 + 2c_1 M_1 c_2 M_2 \cos(\Omega) \cos(\Delta\beta z) \quad (8)$$

assuming that the damping terms are small. For the remaining of the paper, we will focus on $r = 0$ and will define $M_1 = M_1(0)$, $M_2 = M_2(0)$ to simplify notation. Moreover, to simplify arguments, we will stipulate the following normalization condition: $c_1^2 M_1^2 + c_2^2 M_2^2 = 1$ where we have taken $c_m M_m$ to be real, which can always be achieved by a suitable shift of the z or t coordinates.

B. Derivation of the growth equation

If we write the electric field of the q th harmonic as,

$$\vec{E} = \frac{1}{2} \vec{\xi}^{(q\omega)} e^{i[k(q\omega)z - q\omega t]} + \text{c.c} \quad (9)$$

then, within the slowly-varying envelope approximation, the equation for the growth of the amplitude of the q th harmonic becomes,

$$2ik(q\omega)e^{ik(q\omega)z}\frac{d\vec{\xi}^{(q\omega)}}{dz} = -\mu_0(q\omega)^2\vec{P}_{\text{NL}}^{(q\omega)} \quad (10)$$

where $\vec{P}_{\text{NL}}^{(q\omega)}$ is the component of the non-linear polarization oscillating with angular frequency $q\omega$. Now, $\vec{P}_{\text{NL}}^{(q\omega)} = \vec{F}'(I, \epsilon)e^{iq\phi_p(z)}$, where $\vec{F}'(I, \epsilon)$ gives the dependence of the nonlinear response on the intensity and ellipticity of the driving field, and $\phi_p(z)$ is the phase of the driving field of the p th polarization component. We may write $\phi_x(z) = k_1(\omega)z + \psi_x(z)$ and $\phi_y(z) = k_2(\omega)z + \psi_y(z)$, where $\psi_p(z)$ is the additional phase arising from interference of the waveguide modes and $k_m(\omega) = \beta_m(\omega)$ is the waveguide propagation constant for the driving pulse. Henceforth all equations will refer to the q th harmonic, and so in order to avoid clutter we will drop the $(q\omega)$ superscripts. The growth equation for the amplitude of the harmonic for the x- and y- components may then be written in the form,

$$\frac{d\xi_x}{dz} = F_x(I, \epsilon)e^{-i\Delta k_1 z}e^{i\psi_x(z)} = \mathfrak{P}_x \left| \vec{F} \right| e^{i\Psi_x(z)} \quad (11)$$

$$\frac{d\xi_y}{dz} = F_y(I, \epsilon)e^{-i\Delta k_2 z}e^{i\psi_y(z)} = \mathfrak{P}_y \left| \vec{F} \right| e^{i\Psi_y(z)} \quad (12)$$

where Ψ_x and Ψ_y are the total phase for the x- and y- components respectively; \mathfrak{P} is a projection term that relates the nonlinear polarization to x- and y- components of the envelope function, as developed below; $\Delta k_m = k(q\omega) - qk_m(\omega)$; and $\vec{F}(I, \epsilon) = i\mu_0(q\omega)^2\vec{F}'(I, \epsilon)/2k(q\omega)$. We note that, as discussed below, $\vec{F}(I, \epsilon)$ is in general complex since the phase of the nonlinear polarization depends on the trajectory of the ionized electron, and therefore on both the intensity and ellipticity of the driving field. In the equation above, we have factored these phase terms into Ψ_x and Ψ_y .

Considering first the x-polarization, the driving field may be written as,

$$E_x(\vec{r}, z, t) = [c_1 M_1 + c_2 M_2 \cos \Omega e^{-i\Delta\beta z}] e^{i(\beta_1 z - \omega t)} \\ = u_x(z) e^{i(\beta_1 z - \omega t)} \quad (13)$$

where $\Delta\beta = \beta_1 - \beta_2$. Hence we find,

$$\psi_x(z) = \arg[u_x(z)] \\ = \tan^{-1} \left[\frac{-c_2 M_2 \cos \Omega \sin(\Delta\beta z)}{c_1 M_1 + c_2 M_2 \cos \Omega \cos(\Delta\beta z)} \right] \\ \approx -\frac{c_2 M_2}{c_1 M_1} \cos \Omega \sin(\Delta\beta z) \quad (14)$$

where in the last step, the approximation is valid if $|c_1| \gg |c_2|$. Similar considerations show that $\psi_y = 0$ and $\phi_y(z) = \beta_2 z$.

The strength of the nonlinear polarization, $|\vec{F}(I, \epsilon)|$, depends on the intensity and polarization of the driving laser field. Evaluation of $|\vec{F}(I, \epsilon)|$ requires a model of

the interaction of the driving field with the atom, as, for example, developed by Lewenstein et al. [7]. However, for our purposes it is sufficient to assume that the amplitude of the nonlinear polarization, $|\vec{F}|$ can be written in the form:

$$|\vec{F}[I(z), \epsilon(z)]| = AG[I(z)]H[\epsilon(z)] \quad (15)$$

where $A \propto \mu_0(q\omega)^2/2k(q\omega)$ is a constant, $G[I(z)]$ is the intensity-dependent term ranging from $[0, 1]$, and $H[\epsilon(z)]$ is the ellipticity-dependent term ranging from $[0, 1]$.

For the purposes of illustrating the operation of MMP-BQPM it is sufficient to assume that the intensity-dependent term takes the form of a power law $G(I) \approx I^{\eta/2}$. We will assume $\eta \approx 6$, in accordance with earlier work [18, 27, 28]; but note that the broad conclusions of the present paper do not depend strongly on the value of η .

It is also well known that the single-atom efficiency of HHG depends sensitively on the polarization of the driving laser field [29] which arises from the fact that the ionized electron must return to the parent ion in order to emit a harmonic photon. Following the argument given in [21], for a given driving intensity the number of harmonic photons generated as a function of ellipticity maybe approximated by:

$$h(\epsilon) \approx \left(\frac{1 + \epsilon^2}{1 - \epsilon^2} \right)^\mu \quad (16)$$

where $H(\epsilon) = \sqrt{h(\epsilon)}$.

It is predicted that $\mu = q - 1$ within the perturbative regime, as verified [29] by Budil et al. for harmonics $q = 11$ to 19, and by Dietrich et al. for harmonics up to $q \approx 31$ [30]. Schulze et al. found that for higher-order harmonics the sensitivity of harmonic generation to the ellipticity of the driving radiation is lower than predicted by Eqn (16) with $\mu = q - 1$ [31], although in this non-perturbative regime the efficiency of harmonic generation still decreases with ϵ . Further measurements of the dependence of harmonic generation on ϵ have been provided by Sola et al. [32]. It is recognized that Eqn (16) is an approximation, but it will serve our purpose of demonstrating the operation of MMPBQPM.

The offset angle and ellipticity of the harmonics generated by elliptically-polarized radiation have been shown to depend on the ellipticity and intensity of the driving radiation, and on the harmonic order [27, 28, 31, 33, 34]. Propagation effects can also play an important role. Since the amplitude with which harmonics are generated decreases strongly with increasing ellipticity, we are most interested in the ellipticity of the harmonics generated for small ϵ . It has been shown that for higher-order harmonics, and/or high driving intensities, both the ellipticity and change in ellipse orientation of the harmonics generated by radiation with $\epsilon \approx 0$ are close to zero [27]. We will therefore make the simplification that the generated harmonics are linearly polarized along the major axis of

the driving radiation and that we resolve separately the harmonics polarized along the fast and slow axes of the waveguide. Thus, the projection term may be written as:

$$\vec{\mathfrak{P}}(z) = \begin{pmatrix} \cos[\Theta(z)] \\ \sin[\Theta(z)] \end{pmatrix}, \quad (17)$$

and by following the arguments of [21], the coherence lengths for harmonics polarized parallel to the x - and y -axes are different, and hence for a given L_b it is only possible to quasi-phase-match one of these components. Thus, for the remainder of this paper, we will focus on analyzing the harmonics polarized along the x -axis. Therefore, we can approximate $I_q = \xi_x \xi_x^* + \xi_y \xi_y^* \approx \xi_x \xi_x^*$.

Moreover, the phase of the nonlinear polarization depends on the intensity of the driving radiation [35, 36] and its ellipticity [27, 34]. We will ignore the effect of ellipticity on the phase of $\vec{F}(I, \epsilon)$ since, as shown below, harmonic generation is dominated by those regions in which the driving radiation is close to linear polarization. We may write the intensity-dependent phase as a Taylor expansion around I_0 ,

$$\Phi(I) = \Phi(I_0) + \left. \frac{d\Phi}{dI} \right|_{I_0} (I - I_0) + \dots \quad (18)$$

$$\approx \Phi_0 + \nu q (I - I_0). \quad (19)$$

where $\nu = d\Phi/dI|_{I_0}$. For simulations in this paper, we assume $\nu/q \approx 0.2 \text{ rad}/10^{14} \text{ W cm}^{-2}$ based on previous calculations [36].

We may now gather the contributions to the total phase $\Psi_x(z)$:

$$\Psi_x(z) = -\Phi(I_0) - \Delta k_1 z + q\psi_x(z) - q\nu(I - I_0) \quad (20)$$

$$\approx \Psi_0 - \Delta k_1 z - q \frac{c_2 M_2}{c_1 M_1} \cos \Omega \sin(\Delta \beta z) \quad (21)$$

$$- 2q\nu c_1 M_1 c_2 M_2 \cos \Omega \cos(\Delta \beta z) \quad (22)$$

where $\Psi_0 = -\Phi(I_0) - 2q\nu c_1 M_1 c_2 M_2 \cos \Omega$, and the approximation holds if $|c_2| \ll |c_1|$. From Eqns. (12) and (22), we can rewrite the differential equation for the x -component as:

$$\frac{d\xi_x}{dz} = \cos[\Theta(z)] |F[I(z), \epsilon(z)]| e^{+i\Psi_x(z)} \quad (23)$$

$$= A' \Gamma(z) e^{-i\Psi'_x(z)} \quad (24)$$

where

$$A'(z) = A e^{+i\Psi_0} \quad (25)$$

$$\Gamma(z) = \cos[\Theta(z)] |F[I(z), \epsilon(z)]| \quad (26)$$

$$\Psi'_x(z) = -\Psi_x(z) + \Psi_0 \quad (27)$$

$$= \Delta k_1 z + \gamma \sin(\Delta \beta z) + \rho \cos(\Delta \beta z) \quad (28)$$

in which $\gamma = q \frac{c_2 M_2}{c_1 M_1} \cos \Omega$ is the mode interference phase term and $\rho = 2q\nu c_1 M_1 c_2 M_2 \cos \Omega$ is the intensity-dependent phase term.

III. ANALYSIS OF THE GROWTH EQUATION

A. Phase Analysis using the Jacobi-Anger Expansion

The exponential term in Eqn (24) can be expanded into the products of two infinite sums using the Jacobi-Anger Expansion:

$$e^{-i\Psi'_x(z)} = e^{-i\Delta k_1 z} \left[\sum_{l=-\infty}^{+\infty} i^l J_l(-\rho) e^{+il\Delta \beta z} \right] \times \left[\sum_{j=-\infty}^{+\infty} J_j(-\gamma) e^{+ij\Delta \beta z} \right] \quad (29)$$

where J_l and J_j are Bessel functions of the first kind and $l, j \in \mathbb{Z}$. It is insightful to factor terms of constant $\sigma = l + j$ to give:

$$e^{-i\Psi'_x(z)} = e^{-i\Delta k_1 z} \sum_{\sigma=-\infty}^{\infty} U_\sigma e^{i\sigma\Delta \beta z} \quad (30)$$

where

$$U_\sigma = \sum_{l+j=\sigma} i^l J_l(-\rho) J_j(-\gamma). \quad (31)$$

We see that the modulation caused by intensity dependent phase and mode beating can be resolved into harmonics $\sigma\Delta\beta$ of the difference in spatial frequency $\Delta\beta$ of the two modes.

B. Source Amplitude Spatial Fourier Analysis

The analysis above suggests that it would be useful to write the source modulus Γ as a superposition of Fourier components with frequency $\kappa\Delta\beta$ (with $\kappa \in \mathbb{Z}$). For periodic modulation of the driving radiation, the source modulus can be written as a Fourier series:

$$\Gamma(z) = \sum_{\kappa=-\infty}^{\infty} V_\kappa e^{i\kappa\Delta \beta z} \quad (32)$$

and hence the growth differential equation can be written as:

$$\frac{1}{A'} \frac{d\xi_x}{dz} = e^{-i\Delta k_1 z} \sum_{\sigma, \kappa \in \mathbb{Z}} U_\sigma V_\kappa e^{i(\sigma+\kappa)\Delta \beta z}. \quad (33)$$

The terms that contribute to monotonic harmonic growth are those for which the phase is stationary, in other words, $\frac{\partial \Psi_x}{\partial z} = 0$. This implies that for QPM we require $\Delta k_1 = (\sigma + \kappa)\Delta\beta$. We see that the harmonics of the modulation frequency allow QPM of larger wave vector mismatch Δk or, equivalently, of shorter coherence lengths $L_{c,1}$. The fundamental modulation spatial frequency $\Delta\beta$ has a period $2L_b = 2\pi/\Delta\beta$, and hence we may write the QPM condition as $L_b = (\sigma + \kappa)L_{c,1} = nL_{c,1}$,

where $n = \sigma + \kappa$ is the order of the QPM process. Factoring all the terms contributing to monotonic harmonic growth, and ignoring the oscillating terms, the growth equation becomes:

$$\frac{1}{A'} \frac{d\xi_x}{dz} \approx \sum_{\sigma+\kappa=n} U_\sigma V_\kappa \quad (34)$$

for a fixed n , keeping in mind that each of the terms of the sum is complex and may have different signs. Eqn (34) can easily be solved, from which the harmonic intensity is found to be:

$$I_q \approx \frac{1}{2} A' S z^2 \quad (35)$$

where $S = \sum_{\sigma+\kappa=n} U_\sigma V_\kappa$. It is useful to note that the σ and κ terms result from phase and intensity modulation of the driver respectively.

IV. SIMULATION RESULTS

A. Detailed simulations for $L_b = 2L_{c,1}$ and $L_b = L_{c,1}$

To test these ideas, we have conducted a series of simulations. Fig. 1 presents the results of simulations for $L_b = 2L_{c,1}$ ($n = 2$) and three values of Ω and $c_2 M_2$ for $q = 51$ while Fig. 2 presents the same parameters for $L_b = L_{c,1}$ ($n = 1$), $\Omega = 0^\circ$ and two different values of $c_2 M_2$ for $q = 51$. These values are compared against ideal QPM, which is defined by the square wave modulation between zero and one of the harmonic generation with a period of $2nL_{c,1}$.

When $\Omega = 0^\circ$ MMPBQPM is equivalent to “pure MMQPM” since the driving radiation remains linearly polarized at all points within the waveguide; this is seen in Fig. 1-Col (1) where Fig. 1-(1)(b) indicates that modulation of the source term arises from mode-beating alone.

When $\Omega = 90^\circ$, MMPBQPM is equivalent to PBQPM since the mode beating causes the polarization of the driving radiation to beat in an analogous way to PBQPM driven by a linearly polarized beam propagating in a birefringent waveguide. This is seen in Fig. 1-Col (3). More specifically, as seen in Fig. 1- (3)(b), the modulation of the source term is seen to arise from solely polarization beating. It should be noted that for $\Omega = 90^\circ$ the simulations presented here agree with earlier calculations of PBQPM [21]. For intermediate values of Ω (such as in Col (2) where $\Omega = 60^\circ$), modulation of both the intensity and polarization of the driving radiation play a role in QPM.

Fig. 1 also compares the growth of the calculated harmonic intensity with the approximation of Eqn. (35). It can be seen that the approximation agrees closely with the exact calculation, indicating clearly the dominant role played by the terms for which $\sigma + \kappa = n = 2$ as seen in Fig. 1 - Row (a).

Moreover, Fig. 1 - Row (d) maps the values of $U_\sigma V_\kappa$, modulus phase (the terms in the sum in Eqn (34)), as a

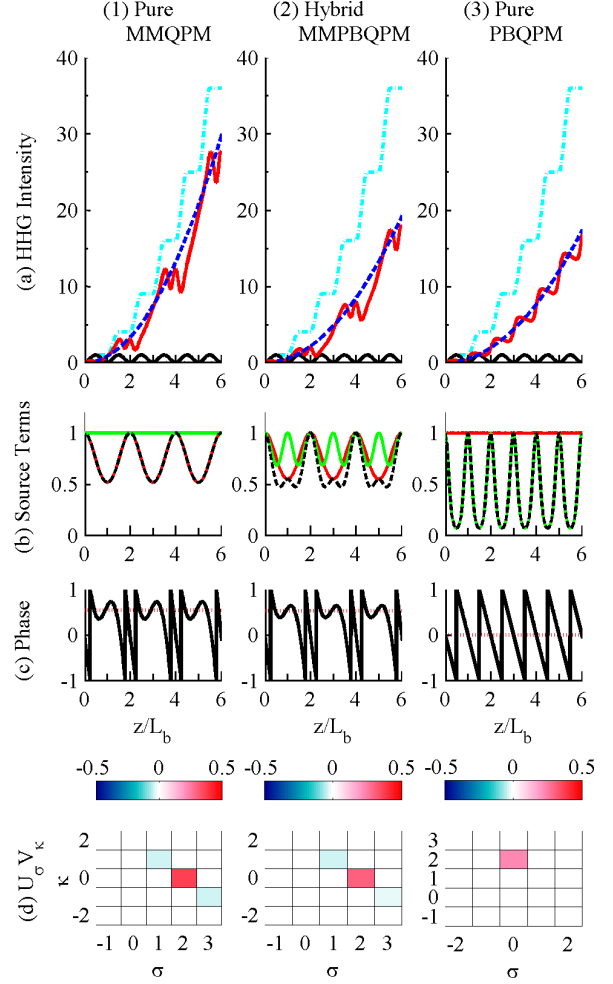


FIG. 1. Simulation results for Columns - (1) “Pure MMQPM” ($c_2 M_2 = 0.002$, $\Omega = 0^\circ$) (2) “Hybrid MMPBQPM” ($c_2 M_2 = 0.01$, $\Omega = 60^\circ$), and (3) “Pure PBQPM” ($c_2 M_2 = 0.05$, $\Omega = 90^\circ$); all for $L_b = 2L_c$ and $q = 51$. Row (a) shows the relative HHG intensity. Dot dashed cyan line shows ideal square wave QPM, solid red line shows the indicated form of MMPBQPM, solid black line shows the intensity for no phase matching, and the dashed blue line shows the harmonic intensity calculated from Eqn (35). Row (b) shows the modulus of the intensity-dependent source term $G[I(z)]$ (solid red line), ellipticity-dependent source term $H[\varepsilon(z)]$ (solid green line), and the combined source terms $|F| = GH$ (dashed black line). Row (c) shows $\Psi_x(z)$, the total phase of $d\xi_x/dz$ (solid black line) and Ψ_x for large z (dotted light red line). Row (d) shows the $U_\sigma V_\kappa$ distribution as a function of σ and κ for $n = \sigma + \kappa$ for $n = 2$

function of σ and κ where $\sigma + \kappa = n$ for a fixed $n = 2$. Hence, only where $\sigma + \kappa = 2$ is $U_\sigma V_\kappa$ is nonzero. For the case of Pure MMQPM, Col (1), and Hybrid MMPBQPM, Col (2), the dominant contributing term is $(\sigma, \kappa) = (2, 0)$ indicating that QPM arises predominantly from phase modulation of the driver, not intensity modulation. This can also be seen in Fig. 1-1c and Fig. 1-2c where the

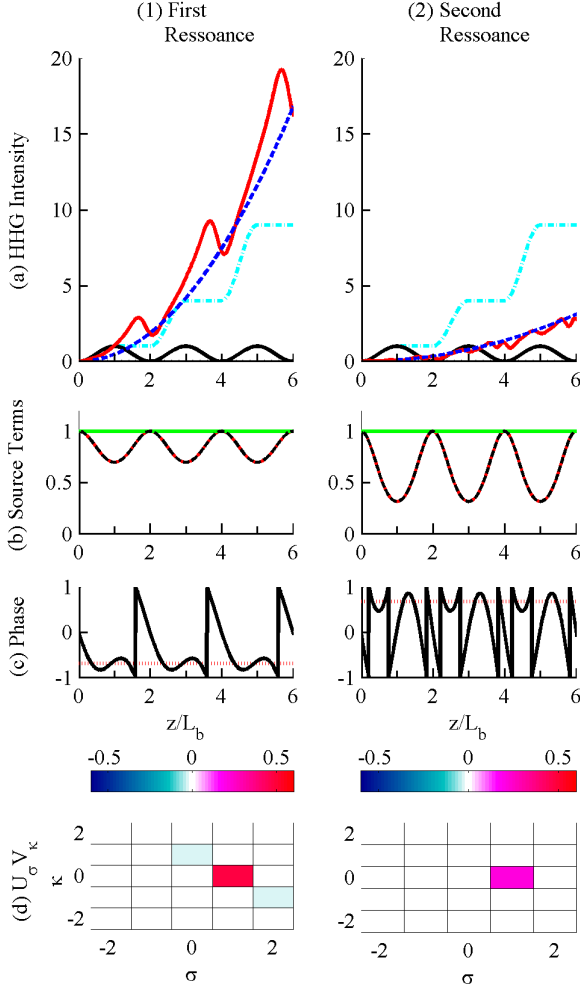


FIG. 2. Simulation results for Columns - (1) the first resonance ($c_2 M_2 = 0.0009$, $\Omega = 0^\circ$) and (2) the second resonance ($c_2 M_2 = 0.0091$, $\Omega = 0^\circ$); all for $L_b = L_c$ and $q = 51$. Row (a) shows the relative HHG intensity. Dot dashed cyan line shows ideal square wave QPM, solid red line shows the indicated form of MMPBQPM, solid black line shows the intensity for no phase matching, and the dashed blue line shows the harmonic intensity calculated from Eqn (35). Row (b) shows the modulus of the intensity-dependent source term $G[I(z)]$ (solid red line), ellipticity-dependent source term $H[\varepsilon(z)]$ (solid green line), and the combined source terms $|F| = GH$ (dashed black line). Row (c) shows $\Psi_x(z)$, the total phase of $d\xi_x/dz$ (solid black line) and Ψ_x for large z (dotted light red line). Row (d) shows the $U_\sigma V_\kappa$ distribution as a function of σ and κ for $n = \sigma + \kappa$ for $n = 1$.

regions of harmonic growth occur for points where the phase Ψ_x is within $\pi/2$ of the phase of ξ_x for large z . In contrast, for the case of Pure PBQPM, Fig. 1 - Col(3), the dominant term is $(\sigma, \kappa) = (0, 2)$. This suggests, as expected, that for Pure PBQPM, phase modulation does not contribute to QPM but only the modulation of the amplitude of the source term caused by polarization beating.

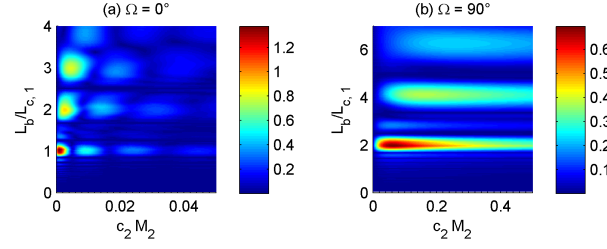


FIG. 3. Relative HHG amplitude $|\xi_x(z)|$ for $q = 51$ at large z ($z = 10L_{c,1}$) as a function of $L_b/L_{c,1}$ and $m = 2$ mode coupling strength $c_2^2 M_2^2$ where $c_1^2 M_1^2 = 1 - c_2^2 M_2^2$, normalized to ideal square wave QPM for: (a) $\Omega = 0^\circ$, and (b) $\Omega = 90^\circ$.

Fig. 2 presents the same parameters in Fig. 1 for $n = 1$ (or $L_b = L_{c,1}$), for two different values of $c_2 M_2$ and $\Omega = 0^\circ$. We see that for both columns, the only terms which contribute are those for which $\sigma + \kappa = 1$, as expected. For Col (1), optimal MMQPM enables harmonics to be generated with intensities greater than for ideal square wave QPM. As indicated in Fig. 2-(1)(c), the region of harmonic growth coincides with Ψ_x being within $\pm\pi/2$ of the phase of ξ_x for large z . Moreover, the largest contributing term of $U_\sigma V_\kappa$ in Fig. 2-(1)(d) is $(\sigma, \kappa) = (1, 0)$; this suggests that QPM is caused primarily by phase modulation, and not by amplitude modulation as reported earlier for MMQPM [16–18]. Moreover, the phase modulation explains why higher growth than ideal square-wave QPM occurs. Fig. 2 - Col (2) shows the output at a different mode mix where $c_2 M_2 = 0.0091$ and $c_1 M_1 = 0.9909$. As discussed below, the mode mixtures for which results are shown in Fig 2 correspond to two of the peaks in a plot of the output of harmonic $q = 51$ as a function of $c_1 M_1$ and $c_2 M_2$.

B. Parameter Space Scans

This section presents a series of parameter space scans for optimizing the harmonic generation by MMPBQPM. In an HHG experiment, pressure, coupling angle Ω , and the mode mix ratio of c_1 to c_2 are parameters that can be adjusted. Pressure tuning equates to tuning the coherence length, or tuning the ratio $L_b/L_{c,1}$ assuming that L_b is fixed for a specific pair of driving and modifying modes.

Fig. 3a shows, for the MMQPM case ($\Omega = 0^\circ$), the variation of the harmonic output as a function of $L_b/L_{c,1}$ and mode mix $c_2 M_2$. Note that here the magnitude of the harmonic amplitude, not intensity, is plotted in order to show more clearly the variation of the harmonic output. As expected, MMQPM is optimized for integer n . Moreover, the peaks shift to increasing $c_2 M_2$ with increasing n . When $n = 1$, the QPM condition becomes $\sigma + \kappa = l + j + \kappa = 1$. The three lowest-order solutions satisfying this condition are $\{l, j, \kappa\} = \{1, 0, 0\}$, $\{0, 1, 0\}$, and $\{0, 0, 1\}$. We therefore expect peaks in the HHG inten-

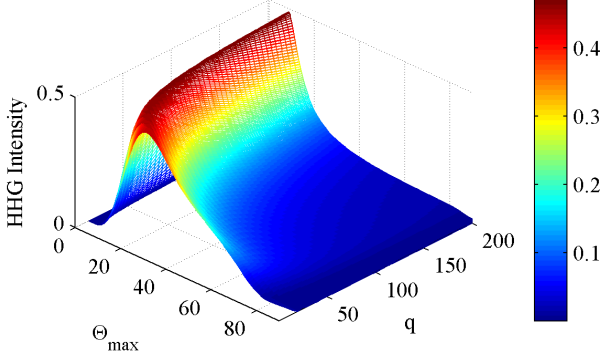


FIG. 4. Relative HHG intensity at $z = L_b$ for $L_b = 2L_{c,1}$ as a function of $\Theta_{max} = \tan^{-1} \left(\frac{c_2 M_2}{c_1 M_1} \right)$ and q , normalized to ideal QPM.

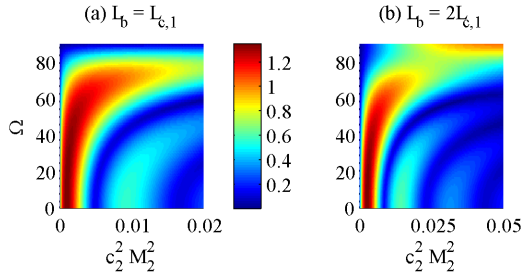


FIG. 5. Relative HHG amplitude for $q = 51$ after $2L_b$ as a function of coupling angle Ω and $m = 2$ mode coupling strength $c_2^2 M_2^2$ where $c_1^2 M_1^2 = 1 - c_2^2 M_2^2$, normalized to ideal QPM for: (a) $L_b = L_{c,1}$, and (b) $L_b = 2L_{c,1}$.

sity to occur for values of $c_2 M_2$ corresponding to peaks in $|J_1(-\rho)J_0(-\gamma)|$, $|J_0(-\rho)J_1(-\gamma)|$, or $|J_0(-\rho)J_0(-\gamma)|$. The maxima along the line $L_b/L_{c,1}$ shown in Fig 3a arise from the variations of $c_2 M_2$ which optimize the functions of $|J_l(-\rho)J_j(-\gamma)|$.

When $n = 2$, $\sigma + \kappa = l + j + \kappa = 2$, and the three lowest order terms are $\{1, 1, 0\}$, $\{0, 1, 1\}$, or $\{1, 0, 1\}$. Thus the values of optimal for $c_2 M_2$ will be around the extrema of $|J_1(-\rho)J_1(-\gamma)|$, $|J_0(-\rho)J_1(-\gamma)|$, $|J_1(-\rho)J_0(-\gamma)|$. Because the positions of the local extremas of the Bessel function increase with increasing $|l|$ or $|j|$, optimal ρ and γ and thus optimal $c_2 M_2$ will increase as well. Therefore, increasing n will result in larger values of $|l|$ and $|j|$ contributing to the harmonic growth corresponding to the Bessel function peaks shifted to higher values of $(-\rho)$ and $(-\gamma)$ and hence higher values of $c_2 M_2$.

Similarly, Fig. 3b shows the PBQPM case where $\Omega = 90^\circ$. As discussed in [21], PBQPM will occur when $L_b = nL_{c,1}$ and n is even – as is evident in Fig. 3b. Since $\Omega = 90^\circ$, $\rho = \gamma = 0$, and since $J_l(0)J_j(0) = 0$ unless $l = j = 0$, monotonic harmonic growth can only occur for $\sigma = l + k = 0$. Hence optimal PBQPM occurs when the Fourier coefficient V_k is large for even κ . Furthermore, PBQPM does not contribute to any phase modulation

because $\sigma = 0$ as seen from Eqn (30). The optimal value of $c_2 M_2$ increases with the order n of QPM since increasing this parameter shifts the Fourier spectrum of the driving intensity modulations to higher orders. The optimal value of $c_2 M_2$ is explored more clearly in Fig. 4, which shows the normalized harmonic intensity for $\Omega = 90^\circ$ as a function of the harmonic order q and the maximum angle $\Theta_{max} = \tan^{-1} \left(\frac{c_2 M_2}{c_1 M_1} \right)$ the major axis of the elliptical driving radiation makes with the x -axis. If Θ_{max} is too close to 0° , then the ellipticity modulation is not enough to suppress the destructive zones. If Θ_{max} is too close to 90° , then the harmonic generation suppression zone is too large to create efficient harmonics.

Fig. 5 plots, for the cases $L_b = L_{c,1}$ and $L_b = 2L_{c,1}$, the calculated relative amplitude at $z = 2L_b$ of the $q = 51$ harmonic as a function of Ω and the relative intensity of the $m = 2$ mode. In the case of Fig. 5a, $L_b = L_{c,1}$, the relative amplitude achieved with “pure MMQPM” (i.e. $\Omega = 0$) is greater than that of ideal square wave QPM as explained above. For $\Omega = 0^\circ$, the intensity oscillates with increasing $c_2 M_2$, with the size of the resonant peaks decreasing with increasing $c_2 M_2$. These resonance peaks are caused by peaks of the products $J_l(-\rho)J_j(-\gamma)$ with ρ and γ being a linear function of $c_2 M_2$ (for small $c_2 M_2$) as explained above. For the case of pure PBQPM, i.e. $\Omega = 90^\circ$ and $L_b = L_{c,1}$, the harmonic intensity is seen to be very low and almost independent of the relative intensity of the two modes since the phase-matching condition for lowest-order PBQPM is not satisfied, and QPM is not achieved.

Lowest-order QPM occurs for $n = 2$, as shown in Fig 5b, a region of bright harmonic generation occurs for $\Omega = 90^\circ$ and $c_2 M_2 \approx 0.04$. When $\Omega = 0^\circ$ the harmonic intensity oscillates in a similar manner to that observed in Fig. 5a.

V. CONCLUSION

We have developed a generalized analysis of MMQPM and PBQPM together with a simplified Fourier analysis which gives additional insights into the dominant contributions of quasi phase-matching. In addition we have shown that PBQPM could be achieved without a birefringent waveguide by exciting a pair of waveguide modes with two orthogonal polarizations.

Our analysis of MMQPM showed, in contrast to our earlier analysis [16, 18], that QPM is dominated by the modulation of phase of the harmonic source term, not of its amplitude. This allows, under optimal conditions, MMQPM to generate harmonics with an intensity greater than possible with ideal, square-wave QPM.

The authors would like to thank the EPSRC for support through grant No. EP/G067694/1. Lewis Liu would like thank David Lloyd for fruitful discussions and the James Buckee Scholarship of Merton College, Oxford for its support.

VI. APS COPYRIGHT NOTICE

Copyright to the [above-listed] unpublished and original article submitted by the [above] author(s), the abstract forming part thereof, and any subsequent errata (collectively, the Article) is hereby transferred to the American Physical Society (APS) for the full term thereof throughout the world, subject to the Author Rights (as hereinafter defined) and to acceptance of the Article for

publication in a journal of APS. This transfer of copyright includes all material to be published as part of the Article (in any medium), including but not limited to tables, figures, graphs, movies, other multimedia files, and all supplemental materials. APS shall have the right to register copyright to the Article in its name as claimant, whether separately or as part of the journal issue or other medium in which the Article is included.

-
- [1] M. Uiberacker and et al, *Nature* **446**, 627 (2007)
 - [2] M. Schultze and et al, *Science* **328**, 1658 (2010)
 - [3] A. Cavalieri and et al, *Nature* **449**, 1029 (2007)
 - [4] R. I. Tobey, M. E. Siemens, O. Cohen, M. M. Murnane, H. C. Kapteyn, and K. A. Nelson, *Optics Letters* **32**(3), 286 (2007)
 - [5] R. L. Sandberg and et al, *Phys. Rev. Lett.* **99**, 098103 (2007)
 - [6] P. B. Corkum, *Phys. Rev. Lett.* **71**(13), 1994 (1993)
 - [7] M. Lewenstein, P. Yu, A. L'Huillier, and P. B. Corkum, *Physical Review A* **49**(3), 2117 (1994)
 - [8] C. G. Durfee, A. R. Rundquist, S. Backus, C. Herne, M. M. Murnane, and H. C. Kapteyn, *Phys. Rev. Lett.* **83**(11), 2187 (1999)
 - [9] A. R. Rundquist, C. G. Durfee, Z. Chang, S. B. C. Herne, M. M. Murnane, and H. C. Kapteyn, *Science* **280**(5368), 1412 (1998)
 - [10] T. Popmintchev and et al, *Science* **8**, 1287 (2012)
 - [11] T. Robinson, K. O'Keeffe, M. Zepf, B. Dromey, and S. M. Hooker, *J. Opt. Soc. Am. B* **27**, 763 (2010)
 - [12] B. Dromey, M. Zepf, M. Landreman, K. O'Keeffe, T. Robinson, and S. M. Hooker, *Applied Optics* **46**, 5142 (2007)
 - [13] J. Peatross, S. Voronov, and I. Prokopovich, *Opt. Express* **1**(5), 114 (1997)
 - [14] A. L. Lytle, X. Zhang, P. Arpin, O. Cohen, M. M. Murnane, and H. C. Kapteyn, *Optics Letters* **33**(2), 174 (2008)
 - [15] X. Zhang, A. L. Lytle, T. Popmintchev, X. Zhou, H. C. Kapteyn, M. M. Murnane, and O. Cohen, *Nature Physics* **3**(4), 270 (2007)
 - [16] M. Zepf, B. Dromey, M. Landreman, P. Foster, and S. M. Hooker, *Phys. Rev. Lett.* **99**, 143901 (2007)
 - [17] T. Robinson, *Quasi-Phase-Matching of High-Harmonic Generation*, D.Phil thesis, University of Oxford (2007)
 - [18] B. Dromey and et al, *Opt. Express* **15**(13), 7894 (2007)
 - [19] D. Walter and et al, *Opt. Express* **14**(6), 3433 (2006)
 - [20] I. Christov, H. Kapteyn, and M. Murnane, *Opt. Express* **7**(11), 362 (2000)
 - [21] L. Z. Liu, K. O'Keeffe, and S. M. Hooker, *Phys. Rev. A* **85**, 053823 (2012)
 - [22] L. Z. Liu, K. O'Keeffe, and S. M. Hooker, *Opt. Lett.* **37**(12), 2415 (2012)
 - [23] L. Z. Liu, K. O'Keeffe, and S. M. Hooker, "High harmonic optical generator [polarization beating]," Isis Innovation, U.K. Patent Application No. GB1117355.6 (07 Oct. 2011)
 - [24] L. Z. Liu, K. O'Keeffe, and S. M. Hooker, "High harmonic optical generator [optical rotation]," Isis Innovation, U.K. Patent Application No. GB1208753.2 (18 May 2012)
 - [25] A. Bahabad and et al, *Nature Photonics* **4**, 570 (2010)
 - [26] P. L. Shkolnikov, A. E. Kaplan, and A. Lago, *J. Opt. Soc. Am. B* **13**(2), 412 (1996)
 - [27] P. Antoine and et al, *Phys. Rev. A* **53**(3), 1725 (1996)
 - [28] P. Antoine and et al, *Phys. Rev. A* **55**(2), 1314 (1997)
 - [29] K. S. Budil, P. Salieres, M. D. Perry, and A. L'huillier, *Phys. Rev. A* **48**(5), R3437 (1993)
 - [30] P. Dietrich and et al, *Phys. Rev. A* **50**(5), 3585 (1994)
 - [31] D. Schulze and et al, *Phys. Rev. A* **57**(4), 3003 (1998)
 - [32] I. J. Sola and et al, *Nature Physics* **2**, 320 (2006)
 - [33] N. L. Manakov and Z. Ovseyannikov, *Sov. Phys. JETP* **52**
 - [34] V. Strelkov and et al, *Phys. Rev. Lett.* **107**, 043902 (2011)
 - [35] M. Lewenstein, P. Salieres, and A. L'Huillier, *Phys. Rev. A* **52**, 4747 (1995)
 - [36] H. J. Shin and et al, *Phys. Rev. A* **63**, 1050 (2001)